Appendix F, Life Cycle Analyses

Attachment F.5 Delta Smelt Life Cycle Model with Entrainment (LCME)

F.5.1 Delta Smelt

F.5.1.1 Delta Smelt Life Cycle Model with Entrainment

Polansky et al. (2021) developed a hierarchical stage-structured state-space life cycle model for Delta Smelt to identify factors with the strongest statistical support for having influence on the species' recruitment and survival. This modeling approach is useful as an ecological modeling tool because it can separate descriptions of state and observation processes and permit the integration of disparate data sets. This Delta Smelt life cycle model was later expanded from four to seven life stages with a component that separately describes the entrainment process at the Sacramento–San Joaquin Delta (Delta) export facilities (Smith et al. 2021). This model produces expected values for larval recruitment and survival at the subsequent life stages. The most statistically supported model variant in Smith et al. (2021) used means of December-June Old and Middle River (OMR) values and June-August outflow aggregated from monthly values or longer timescales; therefore, CalSim output for the scenarios/alternatives can be directly incorporated into the model framework. The most statistically supported model in Smith et al. (2021) also included food/prey metric term during the months of January to March. By using the relationship between zooplankton density and salinity, CalSim-predicted X2 values were then used to estimate the expected change in the food/prey metric for January-March months across alternatives. Reclamation used this model to calculate expected annual population growth rate (λ; the abundance of current year divided by abundance from previous year) for alternative flow scenarios by using CalSim output and subsequent zooplankton model. The metric of interest will be geometric mean of λ for a specified time frame (e.g., 1995-2015), which will be compared across alternatives. For the purpose of this text, Smith et al.'s (2021) model will be referred to as the Delta Smelt Life Cycle Model with Entrainment (LCME).

F.5.1.1.1 Methods, assumptions

The Delta Smelt LCME was run based on flow inputs from CalSim 3. The approach followed the Collaborative Science and Adaptive Management Program (CSAMP) Delta Smelt Structured Decision Making (SDM) process, where historical years (1995-2015) were adjusted according to a CalSim 3 scenario and the geometric mean λ was calculated for each scenario. There is an expectation that zooplankton abundance (i.e., prey item for Delta Smelt) would change based on flow (Kimmerer and Rose 2018), and as such, a zooplankton submodel constructed for the Delta Coordination Group and CSAMP Delta Smelt SDM was applied to the CalSim 3 scenarios. For the zooplankton term, upper and lower 95% confidence intervals were calculated and applied into the analysis to better understand sensitivity of the model output to variation in zooplankton

abundance. We did not update any other model inputs (turbidity, temperature, and predators) due to the complexity and lack of predictive models associated with the other values. Furthermore, it is unclear whether flow changes at a project operations scale meaningfully affect the functioning of the Bay-Delta food web. What is of interest in this analysis is to determine how much the expected long-term abundance of delta smelt might change based on the proposed changes in water management.

Main model

Monthly flow data were pulled from CalSim 3 dss files through R and were summed or averaged depending on the variables for the LCME. OMR flow variables were either extracted directly from CalSim 3 as monthly average value in cfs, or averaged if the timespan covers two months (Table F.5-1). The sum of Delta outflow from June to August were calculated by multiplying the CalSim 3 predicted monthly Net Delta Outflow Index (NDOI-ADD + NDOI-MIN) by the number of days for each month and then added together. The total values in cfs per day were then converted to acre-feet (1 cfs = 1.983 acre-feet per day). Methods and findings of the original application of LCME can be found in Smith et al. (2021). The list of LCME flow variables that were acquired from the CalSim 3 runs can be found in Table F.5-1. R script and data used for the model can be found at (https://github.com/BDO-Science/DeltaSmelt_LCM).

Table F.5-1. List of covariates used in LCME that were replaced with values from CalSim 3 for each alternative.

Life stage	Covariate	Unit	Covariate summary details
Early post-larval (May)	April-May OMR flow	cfs	Mean of the daily sum of tidally filtered flows in the OMRs during April to May
Late post-larval (June)	June-August Outflow	af	Sum of the volume of water moving past a point near the confluence of the Sacramento and San Joaquin rivers, near Pittsburg, California, during June to August
Late post-larval (June)	June OMR flow	cfs	Mean of the daily sum of tidally filtered flows in the OMRs during June
Early subadult (October-November)	December-January OMR flow	cfs	Mean of the daily sum of tidally filtered flows in the OMRs during December to January
Late subadult (January-February)	February OMR flow	cfs	Mean of the daily sum of tidally filtered flows in the OMRs during February
Early adult (March)	March OMR flow	cfs	Mean of the daily sum of tidally filtered flows in the OMRs during March

OMR = Old and Middle River; cfs = cubic feet per second; af = acre-foot.
The Old and Middle River covariates imply entrainment as the mortality mechanism (Smith 2019; Smith et al. 2020). The Delta outflow covariate implies foraging habitat suitability as a suite of mechanisms that align better when outflow is elevated (Smith and Nobriga 2023). The covariates are listed in the order they affect a given cohort in the model.

Assumptions related to the model calibration and new flow inputs

The LCME was parameterized using OMR) flow values derived from the USGS gages and Delta Outflow estimates from DAYFLOW (https://data.cnra.ca.gov/dataset/dayflow), which may differ to some extent with how CalSim 3 calculates these values (OMR and Delta Outflow).

The LCME separately accounts for the influence of OMR and turbidity on delta smelt entrainment. However, the CalSim 3 runs had assumptions built into them about how frequently turbidity triggers that affect OMR would occur. This confounds the turbidity effect on entrainment with the OMR effect in a way that the LCME cannot account for. This may lead to a negative bias in the predicted effect of entrainment; in other words, it may be underestimated somewhat.

The only flow data included in the published LCME (Smith et al. 2021) are OMR and June-August Delta Outflow. In essence, the LCME assumes that these are the most influential flow variables associated with Delta Smelt recruitment and survival. This assumption was supported by Polansky et al. (2021), which is why these flow variables were carried forward and re-tested in the Smith et al. (2021) model.

This analysis consisted of the years 1995 to 2015, so it is unclear how representative model predictions of Delta Smelt population trajectory will be when simulating scenarios that include environmental conditions outside the range of observations the model was fit to. In addition, it is unclear how model parameter estimates and predictions of Delta Smelt population may be affected by climate change impacts and the ongoing and proposed supplementation efforts.

Zooplankton model

To calculate zooplankton abundance/density changes related to changes in flow associated with the CalSim 3 scenarios, Reclamation leveraged the zooplankton abundance estimation process used in the CSAMP Delta Smelt SDM group. To replicate the zooplankton abundance calculation used in the CSAMP Delta Smelt SDM process, estimated X2 values for each month were first retrieved from CalSim 3 dss files. These monthly X2 values were then converted into salinity values for each region defined in the Delta Smelt Individual-Based Model (IBM) (Rose et al. 2013) using a generalized linear model developed by Compass (see Attachment 1, *Maunder and Deriso Revised Model*).

Similar to the CSAMP Delta Smelt SDM process, Generalized Additive Models (GAMs) were constructed to predict the zooplankton density Delta Smelt were expected to spatially overlap with given a salinity level for each IBM region and zooplankton taxon (see Attachment 2, *CVPIA Winter-Run and Spring-Run Life Cycle Models*). Predictor variables for each GAM were the tensor product smooth of the interaction between salinity and day of year, as well as random effects for year and station (when more than one station exists in the dataset). To produce the monthly model output, the 15th of each month was used as the data input.

Once salinity values were calculated for each Delta Smelt IBM region, month, and scenario, expected zooplankton densities were then estimated for every zooplankton taxon, month, region, and scenario using output from the GAMs. Upper and lower 95% confidence intervals from these predictions were calculated through 1,000 independent draws from the model distribution, similar to a bootstrapping process. Just as was done in the CSAMP Delta Smelt SDM process, for each alternative, the initial output was scalar values of the taxa-specific zooplankton density under the particular management conditions divided by the same prediction under baseline/historical conditions. However, because 0 values were present in the baseline, it resulted in infinite values for the scalar calculations. These infinite values were replaced with the maximum finite scalar calculated from model predictions for a specific alternative, taxon, region, and month (across years). When this step still yielded no finite scalar value, the maximum finite scalar value from a given alternative, taxon, and month was used instead.

Because the Delta Smelt IBM and LCME differ in how regions are defined and how zooplankton taxa are grouped, additional conversions were needed. The Delta will continue to be managed as a freshwater ecosystem (i.e., not expected to vary much in terms of salinity) in the near future, and as such, any IBM regions upstream of the Confluence were ignored, and likewise LCME North and South regions were left as is (Figure F.5-1). The Far West LCME region only overlapped with the SW Suisun IBM region and thus, the SW Suisun IBM region results were used to define zooplankton changes in the Far West LCME region. To calculate zooplankton changes in the West LCME region, the following IBM regions were used: NW Suisun, NE Suisun, SE Suisun, Suisun Marsh, and the Confluence. Results from the five IBM regions within the West LCME region were aggregated by multiplying each IBM region's value with the proportion of the region's water volume relative to the total water volume across all five regions. The calculations were as follows:

- Far West LCME region: SW Suisun IBM region (Figure F.5-1)
- West LCME region: (Confluence IBM region x 0.233) + (Suisun Marsh IBM region x 0.174) + (NE Suisun IBM region x 0.110) + (SE Suisun IBM region x 0.220) + (NW Suisun IBM region x 0.264)

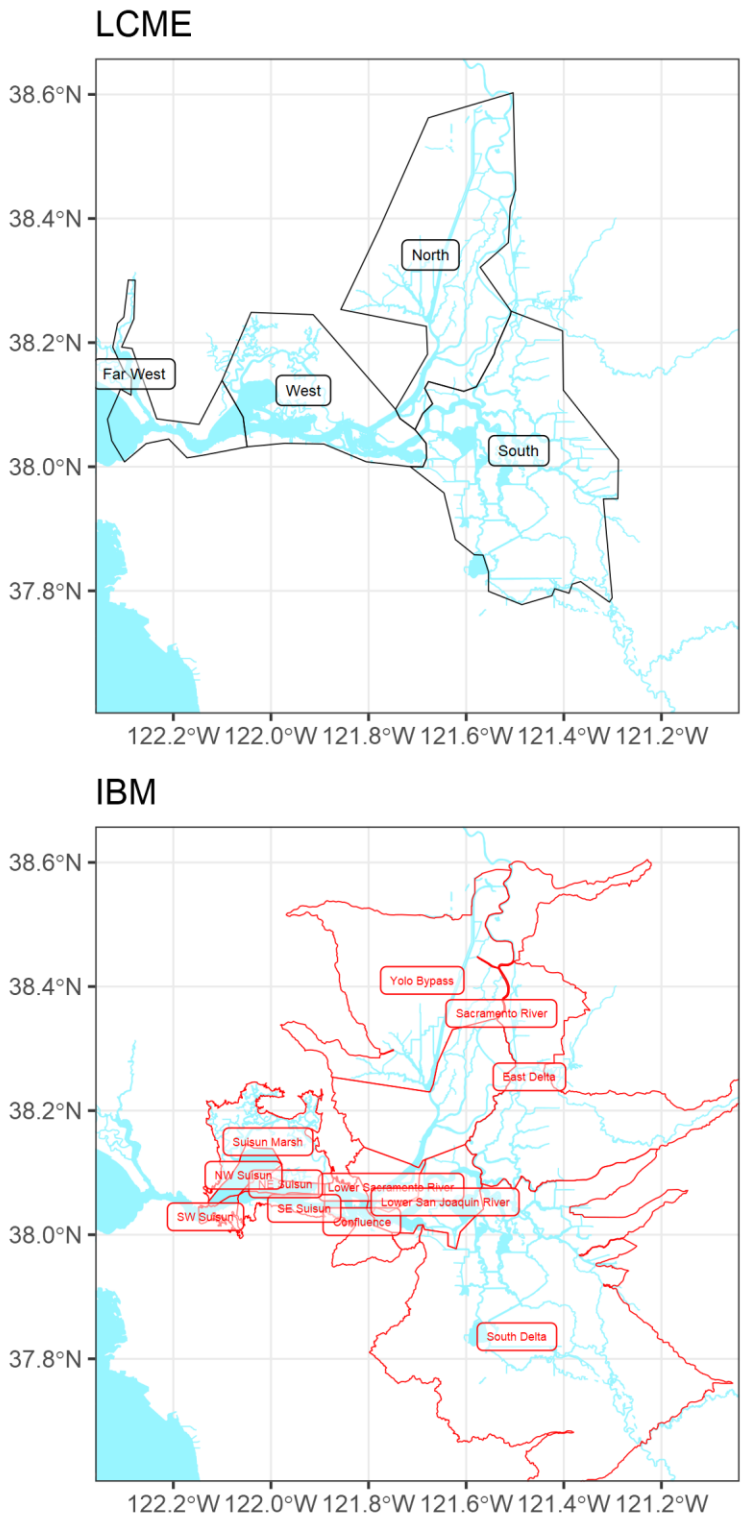

Figure F.5-1. Map of the San Francisco Bay-Delta with LCME regions shown in black (top) and IBM regions shown in red (bottom).

The LCME uses aggregate zooplankton biomass per volume values calculated by summing a number of different zooplankton species and life stages (see Attachment 3, *CVPIA Winter-Run Life Cycle Model*), whereas IBM taxa were more specific, often down to species. Therefore, the proportion of each zooplankton taxa that make up the aggregate zooplankton groups in the LCME data input had to be first estimated for each month and LCME region using raw data provided by the primary authors of the LCME ("ZooMysid_74_19_df.csv"). Using these proportions, the final scalar multiplier values were acquired for the Far West and West LCME regions and zooplankton aggregate groups. In other words, the multiplier scalar values were applied based on the proportion of the particular taxon that make up the prey biomass for a given month and LCME region. For example, if *Pseudodiaptomus forbesi* adults are expected to be twice as abundant and *Eurytemora affinis* adults are expected to be three times as abundant under an alternative, and the two species make up 50% of the biomass each, the final multiplier scalar values will be 2.5 (i.e., [2 x 0.5] + [3 x 0.5]).

These final scalar multipliers were then applied to the LCME aggregated zooplankton dataset ("ZooMysid_74_19_df_median.csv") for the median estimate and the lower and upper 95% confidence interval values (Figure F.5-2). These predictions were then capped at the maximum value that was observed in the LCME aggregated zooplankton dataset ("ZooMysid_74_19_df_median.csv") for the region and month using only data from 1995 to 2019. Lastly, the prey covariates (see Table F.5-3) were acquired by calculating the mean across the four LCME regions.

Table F.5-2. List of taxa analyzed using GAM and the equivalent LCME taxa used to calculate the proportion of each taxon that make up the prey biomass at a given month and LCME region.

GAM response variable	**Taxon definition**	**LCME taxon used to calculate proportion of prey biomass for each month and LCME region**
acartela	*Acartiella sinensis* (copepod) adults	*Acartiella sinensis* (copepod) adults
eurytem	*Eurytemora affinis* (copepod) adults	*Eurytemora affinis* (copepod) adults
pdiapfor	*Pseudodiaptomus forbesi* (copepod) adults	*Pseudodiaptomus forbesi* (copepod) adults
othcalad	Other calanoid copepod adults	Other calanoid adults + *Sinocalanus doerrii* (copepod) adults
othcaljuv	Other calanoid copepodites	Calanoid copepodids + Other calanoid copepodids + *Eurytemora affinis* copepodids + *Sinocalanus doerrii* copepodids + *Pseudodiaptomus* spp. Copepodids + *Acartiella sinensis* copepodids + *Acartia* spp. Copepodids + Diaptomidae copepodids + *Tortanus* spp. copepodids
limno	*Limnoithona* spp. copepods (all stages)	*Limnoithona* spp. + *Limnoithona sinensis* + *Limnoithona tetraspina*
othcyc	Other cyclopoid copepods (all stages)	*Acanthocyclops vernalis*
allcopnaup	Copepod nauplii (all spp.)	Copepod nauplii + Other copepod nauplii + *Eurytemora affinis* nauplii + *Sinocalanus doerrii* nauplii + *Pseudodiaptomus* spp. nauplii
daphnia	*Daphnia* spp. (cladocerans)	*Daphnia* spp. (cladocerans)
othclad	Other cladocerans	*Bosmina longirostris* + *Diaphanosoma* spp. + Other cladocera
other	All other taxa	N/A (model was not used)
mysid	*Hyperacanthomysis longirostris*	*Hyperacanthomysis longirostris* + *Neomysis mercedis*

As zooplankton covariates for natural mortality were only supported for adult life stages (Smith et al. 2021), only zooplankton modeling results from the months of February and March were used as data input for the LCME (Table F.5-3). In other words, a flow effect on delta smelt's food supply is only supported statistically in February-March. The most parsimonious mechanistic explanation is that prey available to adult fish early in the spawning season had a population-scale effect, perhaps by affecting how many eggs could be produced or affecting how many adults survived to spawn a second time. R script and data used for the salinity and zooplankton models can be found at (https://github.com/BDO-Science/DeltaSmelt_LCM).

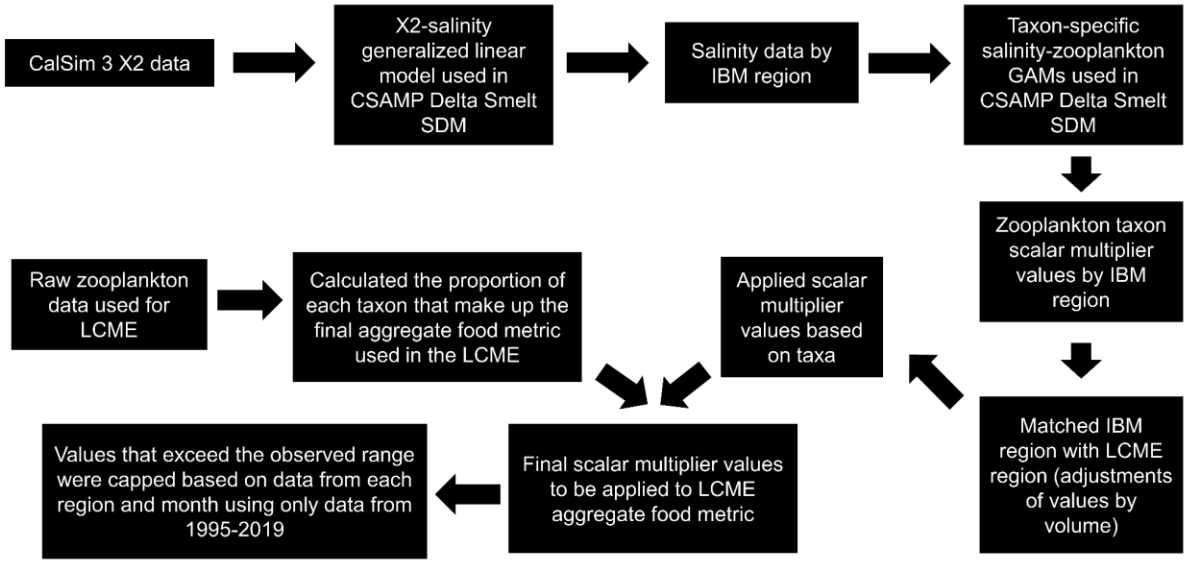

Figure F.5-2. Summary of steps taken to generate estimates of the zooplankton prey density metric for each alternative.

Table F.5-3. List of covariates used in LCME that were replaced with new values based on CalSim 3 and zooplankton model for each alternative.

Life stage	Covariate	Unit	Covariate summary details
Late subadult (January-February)	Food metric for February	Microgram carbon per meter^3	Mean carbon-weighted density of adult calanoid copepods, cyclopoid copepods, cladocerans, and mysid shrimp observed during February zooplankton surveys
Early adult (March)	Food metric for March	Microgram carbon per meter^3	Mean carbon-weighted density of adult calanoid copepods, cyclopoid copepods, cladocerans, and mysid shrimp observed during March zooplankton surveys

The mechanism implied by these prey density covariates is related to food limitation of adult spawners that may affect the number or quality of eggs produced or the number of repeat spawns the fish are able to complete before dying.

Assumptions related to the model calibration and new flow inputs

The zooplankton modeling workflow used salinity to estimate changes in zooplankton biomass related to flow. There are several mechanisms by which a correlation between flow and zooplankton biomass may arise that are not based on salinity *per se* such as transport from upstream, estuarine circulation, etc.

The use of salinity as a covariate also meant that predicted zooplankton biomass at a particular region is static anywhere and everywhere salinity is ≤0.1 ppt salinity, even with additional Delta outflow.

The original purpose of the salinity and zooplankton modeling was to adjust zooplankton data input for the Delta Smelt IBM (Rose et al. 2013; Kimmerer and Rose 2018). As such, there were limitations when the data were converted for the purpose of Delta Smelt LCME (e.g., some missing species and/or life stages in the aggregate LCME zooplankton groups).

F.5.1.1.2 Results

The general statistical prohibition against extrapolation suggests that model predictions are more uncertain when explanatory variables are outside the range of observations to which the model was fit. To visually inspect when the predicted flows and food were outside the observed/empirical range for the LCME, output from CalSim 3 and the zooplankton model were plotted against the empirical data (i.e., data used to estimate parameters in the LCME). See Figure F.5-3 through Figure F.5-5 below. Most CalSim-predicted flows and zooplankton predictions were not outside the range of observations to which LCME was fit, but some alternatives did include out-of-range values. EXP1 included much lower June-August Delta Outflows than observed and higher (more positive) OMR values than observed in some years. EXP3 OMR values were similar to EXP1, but EXP3 June-August Delta Outflows were within the observed range. Alt1, the components of Alt2, and Alt4 contained some April-May OMR values that were more negative than the observed range. Alt1 also contained OMR values more negative than the observed data for the months of December-January and March. Overall, CalSim-predicted June-August Outflow values were generally lower than the DAYFLOW estimates under Wet or Above Normal years (Figure F.5-3, Figure F.5-6). Predicted prey biomass for all alternatives was within the observed range (Figure F.5-5). However, for certain years higher prey biomass than the empirical data were predicted for all alternatives (Figure F.5-3). As a result, mean predicted prey biomass across all alternatives were also higher than the observed data (Figure F.5-5 through Figure F.5-7).

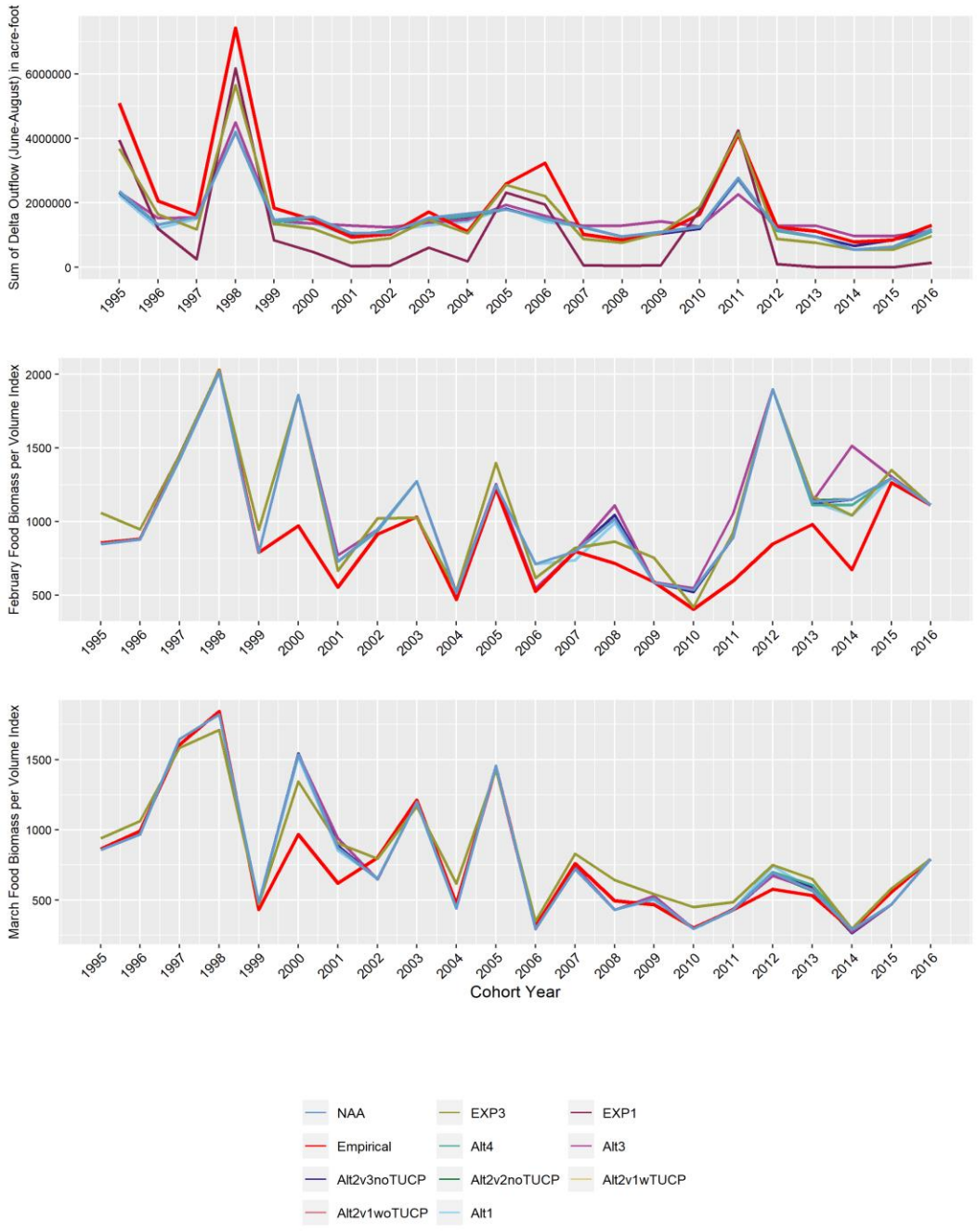

From top to bottom: June-August sum of Delta outflow, February, and March prey metric (biomass per volume) data composed of adult copepods, cladocerans, and mysids. Note that the x-axis represents Delta Smelt cohort year (e.g., February and March prey metric for cohort year 2012 represents data for February and March of 2013).

Figure F.5-3. Annual time series of outflow and prey metric data based on CalSim3 data and salinity-zooplankton model relative to the original dataset used to build the Delta Smelt LCME (labeled as "Empirical").

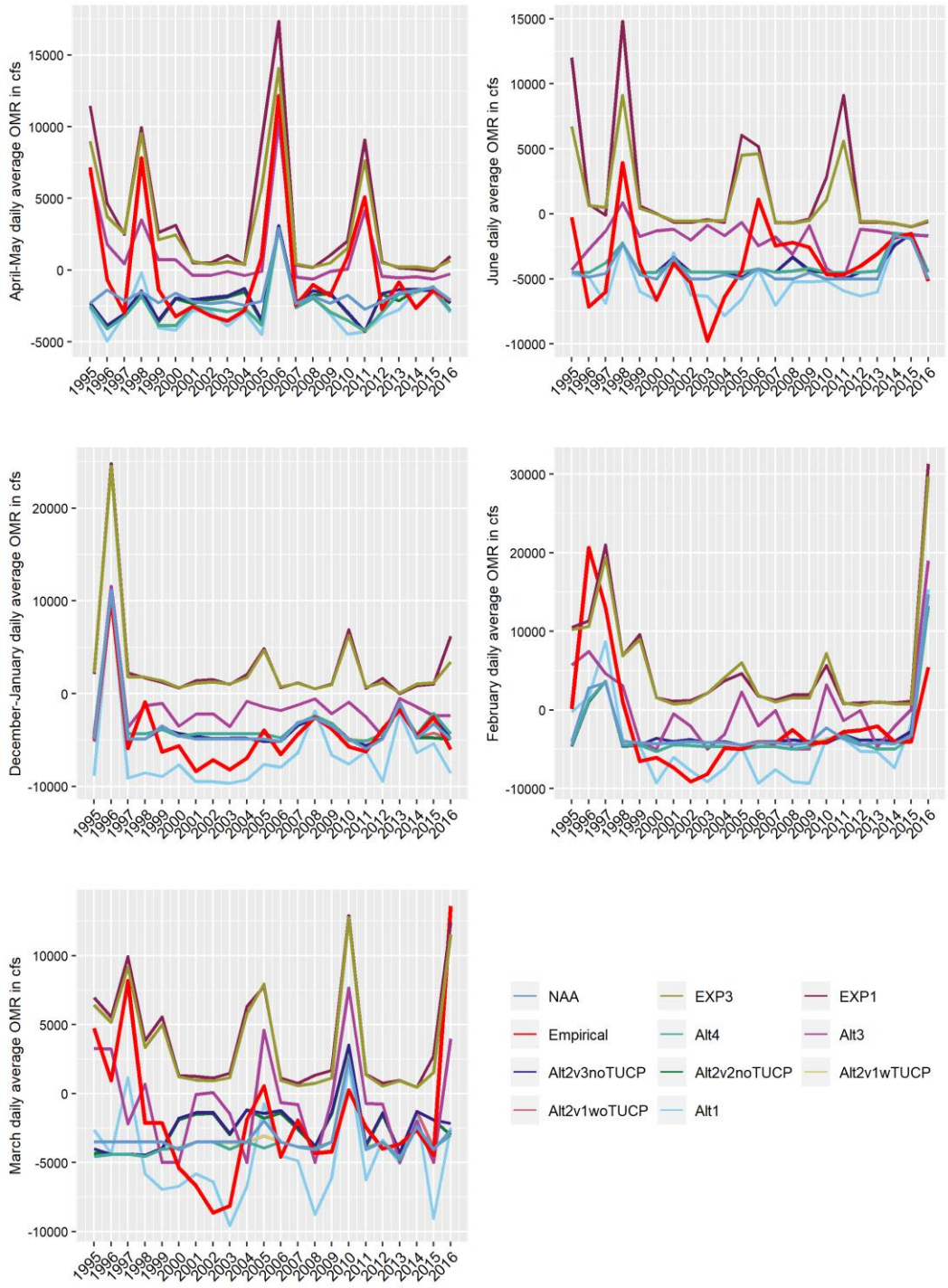

February and March OMR values for cohort year 2012 represents data for February and March of 2013.

Figure F.5-4. Annual time series of monthly average OMR flow data for input to the LCME produced from CalSim3 relative to the original LCME dataset (labeled as "Empirical").

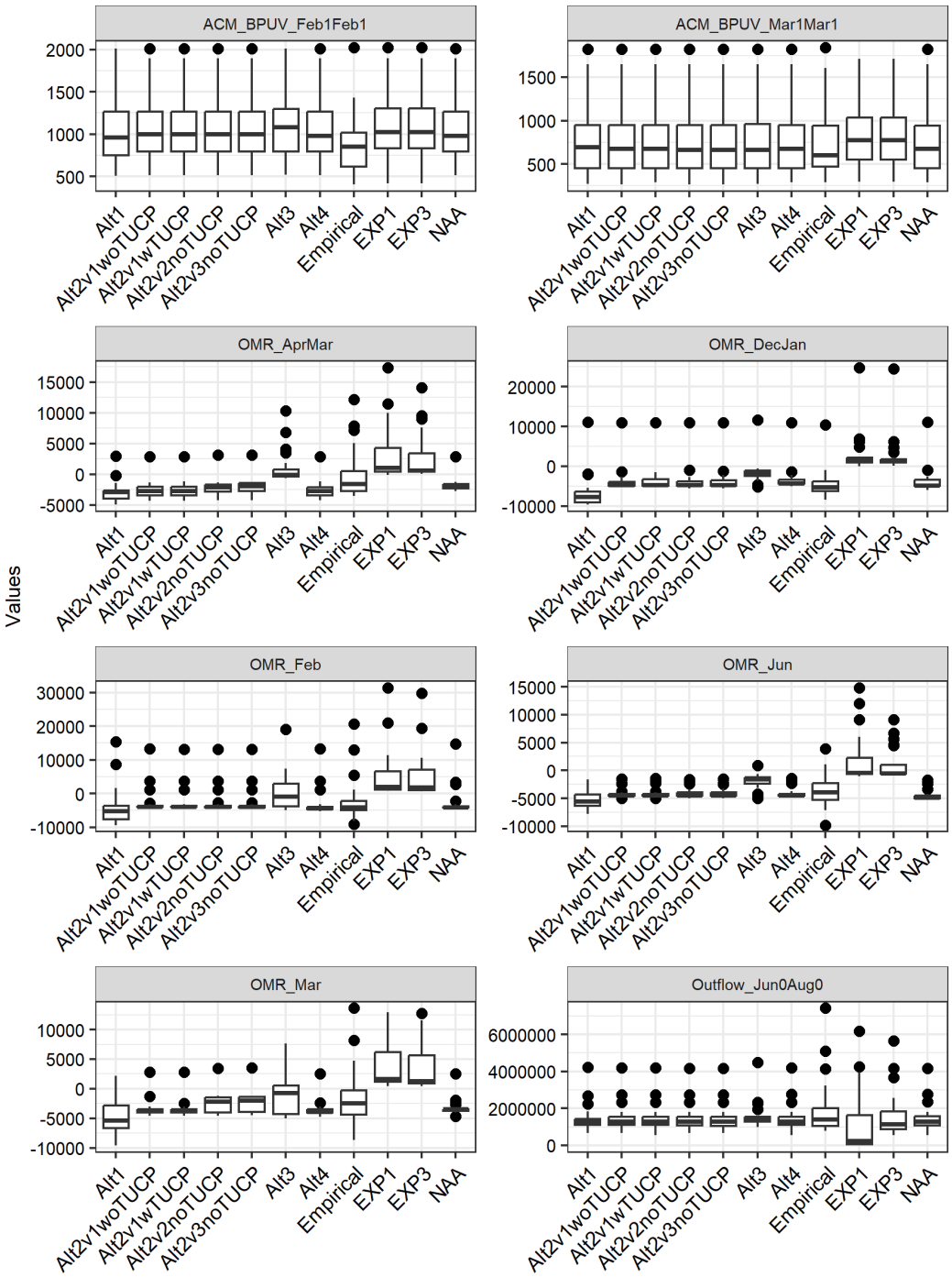

Figure F.5-5. Box plot of covariate values for cohort year 1995 to 2015 sorted by alternative.

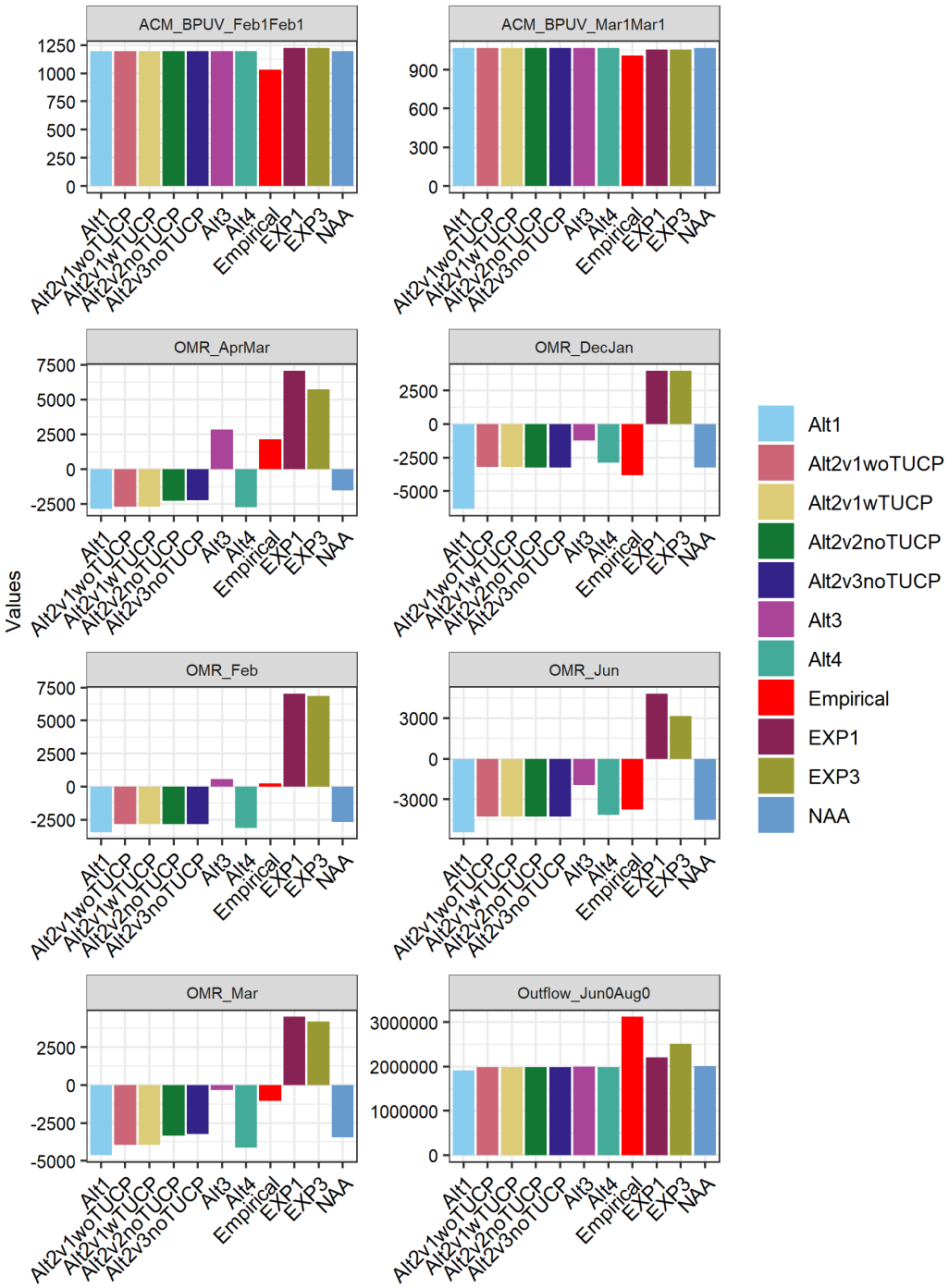

Note that cohort year was matched with the water year that the cohort was born in (e.g., cohort year 1995 = water year 1995).

Figure F.5-6. Mean covariate values used in the LCME for Wet and Above Normal year types.

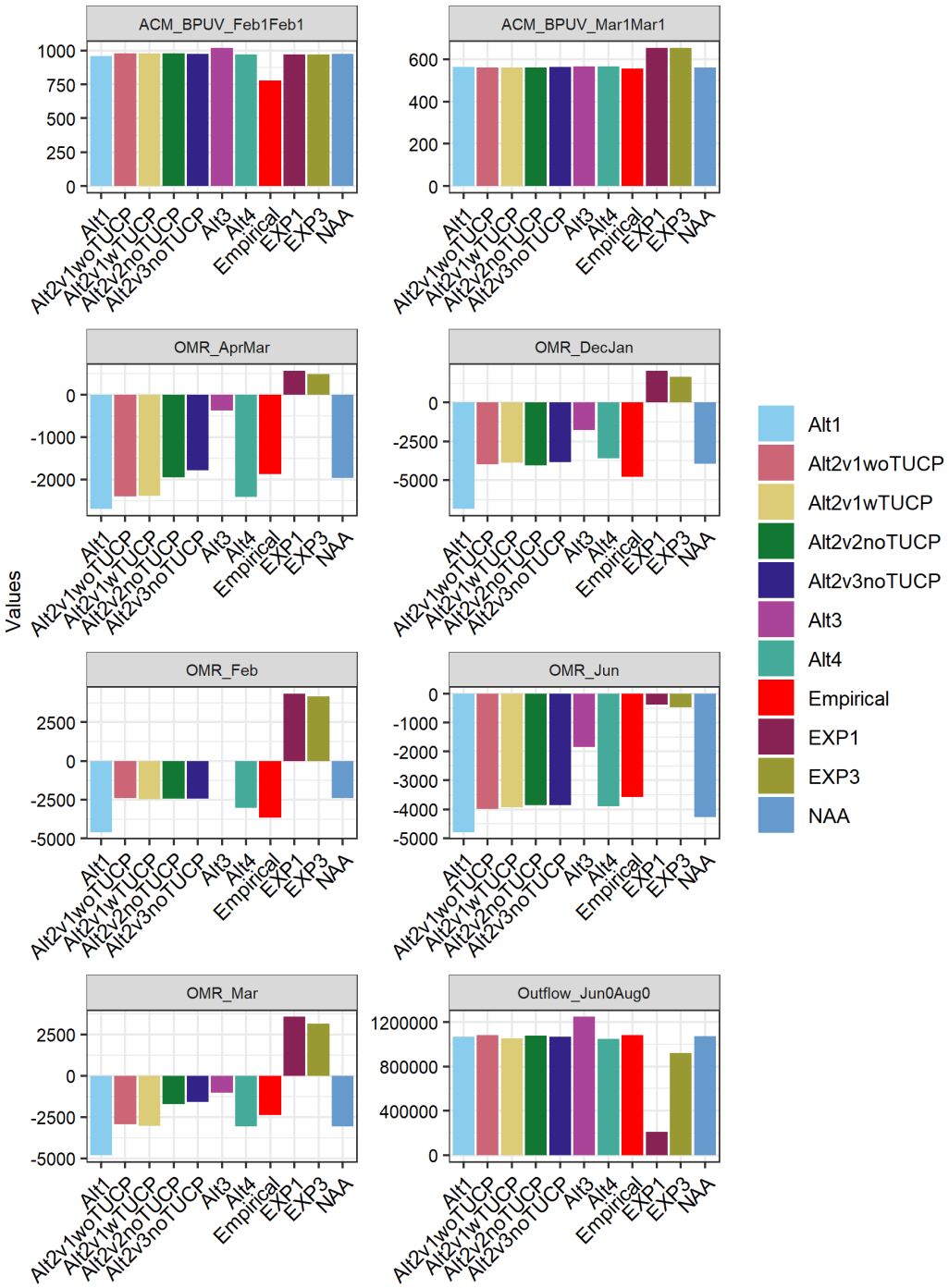

Note that cohort year was matched with the water year that the cohort was born in (e.g., cohort year 1995 = water year 1995).

Figure F.5-7. Mean covariate values used in the LCME for Below Normal, Dry, or Critically Dry year

Estimates of population growth rate (λ; the abundance of current year divided by abundance from previous year) are provided for each cohort year and alternative (Table F.5-4; Figure F.5-8). Generally, dry years showed lower geometric mean λ than wet years (Table F.5-5), and wet years occurred with greater frequency at the beginning of the time series (1995-1999) compared to the end of the time series (2006-2015).

Summarized across all years by calculating the geometric mean of λ for the full 21-year time series (1995-2015), predicted flow and zooplankton conditions associated with EXP3 resulted in the highest mean λ, followed by Alt3 (Figure F.5-9). Meanwhile predicted conditions associated with Alt1 resulted in the lowest value of mean λ. All other alternatives resulted in mean λ between 0.95 and 0.97 (Table F.5-5). Relative to the no action alternative (NAA), Alt3 and EXP3 mean projected λ were the highest among all alternatives, and Alt1 was the lowest (Figure F.5-9). Decomposition of mean λ into time series plots of % change of population growth rate for a given alternative divided by the population growth rate of NAA demonstrated that EXP3- and Alt3-projected λ were greater than NAA in most years (Figure F.5-8). Alt1 projections differed from NAA primarily in the first half of the time series (1995-2005) and were very similar to NAA projections in the latter half of the time series (2006-2015). EXP1-projected λ were relatively greater than NAA in wet years, but less than NAA-projected λ in all other years.

NAA, the various versions of Alt2, and Alt4 performed similarly to the empirical data. While these CalSim-generated scenarios/alternatives resulted in higher λ than the empirical data during dry years, they also resulted in lower λ than the empirical data during wet years (Table F.5-5). The CalSim-generated scenarios/alternatives (NAA, the various versions of Alt2, and Alt4) may have produced higher λ during dry years due to the more positive OMR values for multiple months and higher zooplankton estimates in February (Figure F.5-6). Meanwhile, these same CalSim-generated scenarios/alternatives (NAA, the various versions of Alt2, and Alt4) may have produced lower λ than the empirical data during wet years because of the lower June-August Delta Outflow values and more negative OMR values for certain months (Figure F.5-7).

Table F.5-4. Predicted population growth rate (λ; abundance of current year divided by abundance from previous year) for each cohort year by alternatives.

Year	Empirical	Alt1	Alt2v1 wTUCP	Alt2v1 woTUCP	Alt2v2 noTUCP	Alt2v3 noTUCP	Alt3	Alt4	EXP1	EXP3	NAA	Sacramento Valley Water Year Index
1995	3.56	1.63	1.78	1.79	1.80	1.78	2.25	1.84	4.25	4.05	1.86	Wet
1996	1.37	0.66	0.64	0.64	0.65	0.65	1.06	0.64	1.04	1.27	0.73	Wet
1997	0.68	0.38	0.56	0.57	0.57	0.57	0.78	0.59	0.57	0.99	0.59	Wet
1998	4.78	1.75	1.70	1.67	1.68	1.68	3.03	1.73	5.15	4.88	1.82	Wet
1999	0.79	0.56	0.69	0.70	0.68	0.70	0.89	0.69	0.94	1.27	0.79	Wet
2000	0.69	0.45	0.83	0.83	0.88	0.89	0.81	0.78	0.79	1.17	0.90	Above Normal
2001	0.11	0.12	0.30	0.30	0.33	0.34	0.50	0.30	0.32	0.53	0.31	Dry
2002	0.55	0.68	0.94	0.96	1.04	1.03	1.24	0.94	0.69	1.16	0.93	Dry
2003	0.87	0.71	1.45	1.46	1.54	1.54	1.58	1.45	1.36	2.12	1.51	Above Normal
2004	0.44	0.46	0.84	0.84	0.87	0.87	0.97	0.83	0.53	0.91	0.87	Below Normal
2005	1.94	1.04	1.27	1.27	1.34	1.36	1.58	1.28	2.66	2.85	1.31	Above Normal
2006	3.37	2.04	2.31	2.35	2.40	2.45	2.58	2.29	3.34	3.67	2.41	Wet
2007	0.51	0.33	0.57	0.57	0.58	0.57	0.83	0.53	0.46	0.77	0.57	Dry
2008	0.95	1.00	1.10	1.10	1.17	1.18	1.50	1.07	0.70	1.11	1.09	Critically Dry
2009	0.64	0.45	0.68	0.68	0.68	0.67	0.76	0.66	0.54	1.02	0.67	Dry
2010	1.26	1.31	1.45	1.45	1.47	1.43	1.66	1.46	1.87	1.97	1.48	Below Normal
2011	3.65	3.14	3.26	3.24	3.24	3.25	3.13	3.28	5.57	5.47	3.23	Wet
2012	0.95	0.74	0.98	0.99	1.00	1.00	1.15	1.00	0.67	1.10	1.02	Below Normal
2013	0.90	0.87	0.88	0.88	0.87	0.86	1.04	0.87	0.50	0.83	0.87	Dry
2014	0.43	0.43	0.48	0.52	0.51	0.52	0.71	0.46	0.38	0.57	0.47	Critically Dry
2015	0.66	0.65	0.56	0.63	0.63	0.63	0.74	0.56	0.41	0.60	0.56	Critically Dry

Empirical indicates the observed data used by the LCME.

Table F.5-5. Geometric mean of predicted population growth rate (λ) across all years and binned into wetter and drier years for all alternatives.

Category	Alt1	Alt2v1 woTUCP	Alt2v1 wTUCP	Alt2v2 noTUCP	Alt2v3 noTUCP	Alt3	Alt4	EXP1	EXP3	Empirical	NAA
1995-2015	0.72	0.95	0.94	0.98	0.98	1.20	0.94	1.01	1.41	0.96	0.97
Below Normal, Dry, or Critically Dry years	0.54	0.75	0.74	0.77	0.77	0.95	0.72	0.57	0.90	0.58	0.74
Wet and Above Normal years	0.98	1.24	1.24	1.27	1.28	1.55	1.25	1.91	2.32	1.68	1.32

Empirical scenario indicates the LCME fit to observed data, while all alternative models represent simulations using CalSim output.

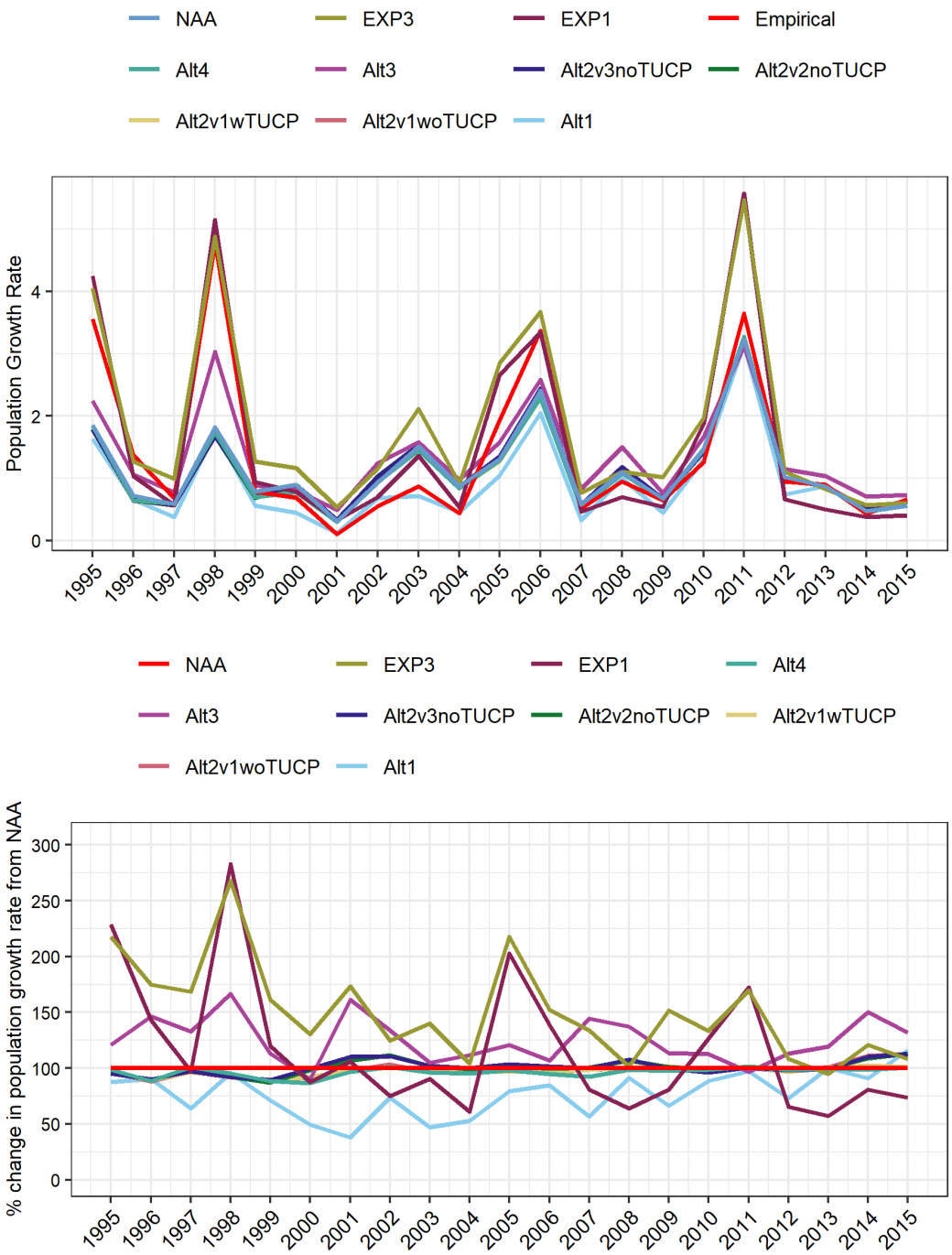

Bottom: Line plot showing % change calculated as λ for a given alternative divided by estimated population growth rate for NAA (no action alternative); no change from NAA = 100. Note the color change for NAA in the bottom figure.

Figure F.5-8. Annual time series of delta smelt population growth rate. Top: Line plot of population growth rate (λ) across alternatives as seen in Table F.5-4.

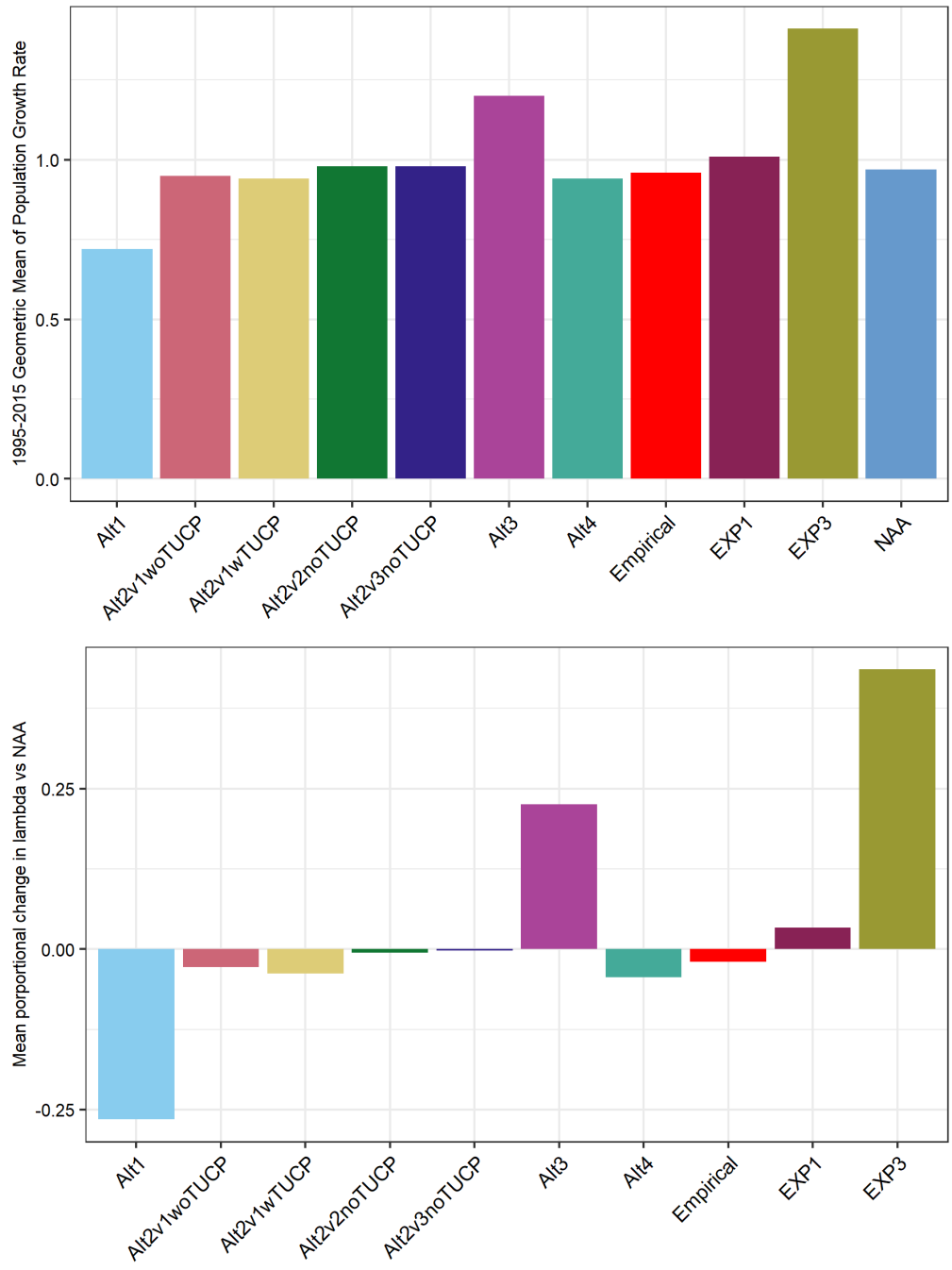

Bottom: Bar plot demonstrating the relative difference in geometric mean of population growth rate (1995-2015) for each alternative compared to the no action alternative ($[\lambda_{alternative} - \lambda_{no\ action}]/\lambda_{no\ action}$). Negative numbers indicate alternatives that result in poorer conditions for delta smelt and positive numbers indicate alternatives that are predicted to improve conditions.

F.5.1.1.3 Figure F.5-9. Mean population growth rates aggregated across the years. Top: Bar plot demonstrating the geometric mean of population growth rate (lambda)

from 1995 to 2015 for the various alternatives as seen in Table F.5-4.Key Takeaways

- Geometric mean of population growth rate from 1995 to 2015 only showed considerable differences from the observed data and/or NAA for EXP3, Alt1, and Alt3 scenarios, where EXP3 and Alt3 performed better than most scenarios/alternatives (i.e., higher λ) and Alt1 performed worse than most alternatives (i.e., lower λ).
- EXP3 and Alt3 scenarios likely produced in higher λ due to more positive OMR flows for most months and the relatively high June-August Delta Outflow during dry years (Figure F.5-5, Figure F.5-6).
- Alt1 scenario likely produced lower λ relative to most scenarios due to the more negative OMR flows during most months (Figure F.5-5, Figure F.5-6).
- NAA, all components of Alt2, and Alt4 did not produce considerably higher λ than the empirical data despite OMR restrictions that should reduce entrainment. This may be due to the apparent trade-off between OMR flow and summer Delta outflow that somehow occurred between these alternatives and the empirical data (Figure F.5-3, 4Figure F.5-4).

F.5.1.1.4 Biological Assessment Takeaways

The Delta Smelt LCME Analysis, Appendix F, *Alternatives Modeling*, Attachment X produces estimates values for larval recruitment and survival at the subsequent life stages (Smith et al. 2021). The most statistically supported model used means of December-June OMR values, June-August outflow aggregated from monthly values or longer timescales, and aggregated food/prey metric from January to March. The model is used to calculate expected annual population growth rate (λ; the abundance of current year divided by abundance from previous year) as a performance measure of Delta seasonal flow operations influence on OMR and outflow over a twenty year time period (1995-2015).

The general statistical prohibition against extrapolation suggests that model predictions are more uncertain when explanatory variables are outside the range of observations to which the model was fit. Most CalSim-predicted flows and zooplankton predictions were not outside the range of observations to which the Delta smelt LCME was fit, but some alternatives did include out-of-range values. EXP1 included much lower June-August Delta Outflows than observed and higher (more positive) OMR values than observed in some years. EXP3 OMR values were similar to EXP1, but EXP3 June-August Delta Outflows were within the observed range. The multiple components of the PA also contained some April-May OMR values that were more negative than the observed range. Overall, CalSim-predicted June-August Outflow values were generally lower than the empirical data under Wet or Above Normal years. Predicted prey biomass for all alternatives was within the observed range, except for certain years where higher prey biomass were predicted than the empirical data for all alternatives.

The geometric mean of the expected population growth across years (1995-2015), λ, for the PA components ranged from 0.95 to 0.98 (Table F.5-6). The means of the expected population growth rate varied more widely across water year types and showed positive growth rates under wetter meteorology and negative growth rates under drier meteorology. Note that wetter years also occurred with greater frequency at the beginning of the time series (1995-1999) compared to

the end of the time series (2006-2015). Predicted flow and zooplankton conditions associated with EXP3 resulted in the highest geometric mean λ (1.30), whereas NAA and the various components of PA produced geometric mean λ similar to the empirical data (0.95-0.98 vs. 0.96). While NAA and the various components of the PA resulted in higher λ than the empirical data during drier years, they also resulted in lower λ than the empirical data during wetter years (Table F.5-6).

NAA and the various components of the PA may have produced higher λ during drier years due to the more positive OMR values for multiple months and higher zooplankton estimates in February. Meanwhile, NAA and the PA components may have produced lower λ than the empirical data during wetter years because of the lower June-August Delta Outflow values and more negative OMR values for some months. NAA and the PA components did not produce higher λ despite OMR restrictions that should reduce entrainment of Delta smelt. This may be due to the apparent trade-off between OMR flow and summer Delta outflow that somehow occurred between PA components and the empirical data (Figures BA2, BA3).

Table F.5-6. Geometric mean of predicted population growth rate (λ) across all years and binned into wetter and drier years for all alternatives.

Category	EXP1	EXP3	NAA	PAwoTUCP woVA	PAwoTUCP wDeltaVA	PAwoTUCP wSystemwideVA	Empirical
1995-2015	1.01	1.41	0.97	0.95	0.98	0.98	0.96
Below Normal, Dry, or Critically Dry years	0.57	0.90	0.74	0.75	0.77	0.77	0.58
Wet and Above Normal years	1.91	2.32	1.32	1.24	1.27	1.28	1.68

Empirical scenario indicates the LCME fit to observed data, while all alternative models represent simulations using CalSim output.

F.5.1.1.5 Environmental Impact Statement Takeaways

Table F.5-7. Geometric mean of predicted population growth rate (λ) across all years and binned into wetter and drier years for all alternatives.

Category	Alt1	Alt2woTUCP woVA	Alt2wTUCP woVA	Alt2woTUCP wDeltaVA	Alt2woTUCP wSystemwideVA	Alt3	Alt4	Empirical	NAA
1995-2015	0.72	0.95	0.94	0.98	0.98	1.20	0.94	0.96	0.97
Below Normal, Dry, or Critically Dry years	0.54	0.75	0.74	0.77	0.77	0.95	0.72	0.58	0.74
Wet and Above Normal years	0.98	1.24	1.24	1.27	1.28	1.55	1.25	1.68	1.32

Empirical scenario indicates the LCME fit to observed data, while all alternative models represent simulations using CalSim output.

F.5.2 References

Kimmerer, W. J., and K. A. Rose. 2018. Individual-Based Modeling of Delta Smelt Population Dynamics in the Upper San Francisco Estuary III. Effects of Entrainment Mortality and Changes in Prey. *Transactions of the American Fish Society* 147(1):223–243. Available: https://doi.org/10.1002/tafs.10015.

Polansky, L., K. B. Newman, and L. Mitchell. 2021. Improving inference for nonlinear state-space models of animal population dynamics given biased sequential life stage data. *Biometrics* 77(1):352–361. Available: https://doi.org/10.1111/biom.13267.

Rose, K. A., W. J. Kimmerer, K. P. Edwards, and W. A. Bennett. 2013. Individual-based modeling of delta smelt population dynamics in the upper San Francisco estuary: I. model description and baseline results. *Transactions of the American Fish Society* 142(5):1238–1259. Available: https://doi.org/10.1080/00028487.2013.799518.

Smith, W. E. 2019. Integration of transport, survival, and sampling efficiency in a model of south delta entrainment. *San Francisco Estuary Watershed Science* 17(4). Available: https://doi.org/10.15447/sfews.2019v17iss4art4.

Smith, W. E., K. B. Newman, and L. Mitchell. 2020. A bayesian hierarchical model of postlarval delta smelt entrainment: Integrating transport, length composition, and sampling efficiency in estimates of loss. *Canadian Journal of Fisheries and Aquatic Sciences* 77(5):789–813. Available: https://doi.org/10.1139/cjfas-2019-0148.

Smith, W. E., and M. L. Nobriga. 2023. A bioenergetics-based index of habitat suitability: spatial dynamics of foraging constraints and food limitation for a rare estuarine fish. *Transactions of the American Fish Society*. Available: https://doi.org/10.1002/tafs.10427.

Smith, W. E., L. Polansky, and M. L. Nobriga. 2021. Disentangling risks to an endangered fish: Using a state-space life cycle model to separate natural mortality from anthropogenic losses. *Canadian Journal of Fisheries and Aquatic Science* 78(8):1008–1029. Available: https://doi.org/10.1139/cjfas-2020-0251.